AN ULTRA-LOW EMITTANCE DESIGN FOR ENERGY RECOVERY LINAC (ERL) INJECTOR

Jun Yamazaki#, ISSP, University of Tokyo, Kashiwa, Chiba 277-8581, Japan
Atsushi Enomoto, Yukihide Kamiya, KEK, Tsukuba, Ibaraki 305-0801, Japan.

Abstract

One of the most important issues concerning energy recovery linac (ERL) [1, 2] injectors is the generation of electron beams with ultra-low emittance and the acceleration of those beams through the injectors without emittance growth [3]. For this purpose, we have developed an efficient simulation code to investigate the mechanism of emittance growth due to the space charge effect and to exploit methods for its suppression [4, 5]. The developed code was used to optimize the parameters of a 5-MeV injector. In the simulation, it was assumed that the voltage of the DC electron gun was 330 kV and the shape of the initial particle distribution at the exit of the gun a uniform ellipse. Even for a gun with voltage as low as that mentioned above, we found that it was possible to attain minimum values of 0.10 μm and 0.83 mm for the rms normalized emittance and the rms bunch length, respectively.

METHOD OF SIMULATION

We developed a simulation code to generate an ultra-low emittance beam in the energy recovery linac (ERL) injector. Serafini and Rosenzweig have discussed a method for the suppression of emittance growth by considering envelopes of bunch slices (Fig. 1) [1]. Using the slice concept and further considering the longitudinal motions, we could account for the space charge effect caused by the changes in velocity more accurately. The initial particle distribution at the exit of the gun in the *rr′* phase space is usually needle-shaped; that is, the phase ellipses of every slice have similar orientations. However, the phase ellipses will have different orientations while passing through the injector, because the space charge fields of each phase ellipse are different. Therefore, there is an increase in the phase space occupied by all the slices.

In order to evaluate the degree of overlap of the slices in the *rr′* phase space, we introduced a "correlation coefficient" in the *aa′* space. Here, *a* is the envelope radius of the slices and *a′* is its derivative with respect to the longitudinal direction. When the correlation coefficient is zero, the ellipses of the slices have similar orientation, and the total emittance projected in the longitudinal direction is minimum.

To calculate *a*, we solved the envelope equations for macro-particles distributed inside the bunch. The longitudinal motions of the macro particles were calculated to obtain their kinetic energies and longitudinal positions. The space charge fields were then calculated by using the particle-in-cell (PIC) method.

#yamazaki@issp.u-tokyo.ac.jp

We used 10^2 for the number of cells, and 10^4 macro-particles were typically employed to suppress numerical noise. To save on computing time, we calculated the slice envelopes only for the tagged particles, which constituted one-tenth of the total number of macro-particles (Fig. 2).

We calculated the space charge densities using only the largest envelopes in the cell, because a uniform density is assumed at each longitudinal location in the envelope equation; even when space charge force was calculated using the average envelope in the cell, there was no significant difference in the final result. The formulae used in this simulation are described in the subsequent sections.

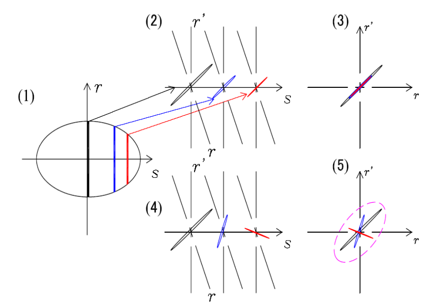

Figure 1 : Slices and phase spaces.

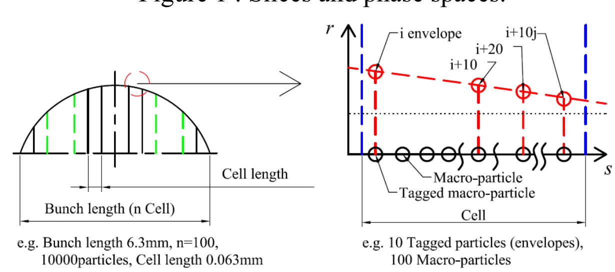

Figure 2 : Cell, particle, and envelope.

Longitudinal Dynamics

The longitudinal motions of macro-particles were calculated using the following differential equations [6],

$$
\begin{aligned}
dt/ds &= 1/c\beta \\
dW/ds &= +e\left(E_{RF,z} + E_{long}\right) .
\end{aligned}
\tag{1}
$$

Here *s* is the longitudinal coordinate of the macro-particles; *t,* the travel time from the gun exit; *W,* the kinetic energy; *e,* the electron charge; *c,* the velocity of light; *β,* the electron velocity divided by *c*; and *γ,* the Lorentz factor. $E_{RF,z}$ and E_{long} are the longitudinal electric fields of RF and space charge, respectively.

Transverse Dynamics

The transverse motions of tagged particles were calculated using the envelope equations [6],

$$\frac{d^2a}{ds^2}+\frac{\gamma'}{\beta^2\gamma}\frac{da}{ds}+(k-K)a-\frac{\varepsilon^2}{a^3}=0 \tag{2}$$

, where

$$k=-\frac{q}{m_0\gamma(c\beta)^2}\left(E_r-c\beta B_\theta\right)\ . \tag{3}$$

a is the slice envelope. k represents both k-values of the solenoid magnetic field [6] and the RF field Eq. 3, K k-value of a space charge field Eq. 4, ε the initial un-normalized emittance. E_r and B_θ radial electric and azimuthal magnetic field of RF respectively.

Space Charge Field

The expressions for longitudinal and radial fields of space charge are given below [5, 7].

$$E_{long}(s)=\frac{1}{2\varepsilon_0}\int\gamma(s_1)ds_1\rho(s_1)\,\mathrm{sgn}(s-s_1)\times\left(1-\frac{\gamma(s_1)|s-s_1|}{\sqrt{a(s_1)^2+\gamma(s_1)^2|s-s_1|^2}}\right) \tag{4}$$

$$E_{Trans,n}(s)=\frac{a(s)}{4\varepsilon_0}\int\gamma(s_1)ds_1\rho(s_1)a(s_1)^2\times\left(\frac{1}{\sqrt{a(s_1)^2+\gamma(s_1)^2|s-s_1|^2}}\right)^3=\frac{a(s)}{4\varepsilon_0}I(s) \tag{5}$$

, where

$$K=\frac{\pi I}{I_0(\beta\gamma)^2}\ .$$

Here *sgn* is the sign function; I_0, the Alfven current (17000 A for electrons); I, the peak current; and ρ, the charge density.

CORRELATION COEFFICIENT

We define the correlation coefficient, *Cor*, as follows,

$$Cor=\frac{\beta\gamma}{4N}\sqrt{\sum_{i=1}^{N}a^2\sum_{i=1}^{N}a'^2-\left(\sum_{i=1}^{N}aa'\right)^2} \tag{6}$$

, where N is the number of tagged particles [4, 5]. In a linear approximation, a is given as $\sqrt{\varepsilon\beta_{Twiss}}$ and a' as $-\alpha_{Twiss}\sqrt{\varepsilon/\beta_{Twiss}}$ [6]. Here, α_{twiss}, β_{twiss}, and γ_{twiss} are Twiss parameters and ε is the emittance. For large values of α_{twiss} (e.g., greater than 100), the slope of ellipse $\gamma_{Twiss}/\beta_{Twiss}$ is nearly equal to a'/a,

$$-\frac{\gamma_{Twiss}}{\beta_{Twiss}}\cong-\frac{\alpha_{Twiss}}{\beta_{Twiss}}=\frac{a'}{a}\ . \tag{7}$$

Therefore, we can optimize the total emittance by using correlation coefficients [5].

INJECTOR DESIGN

The injector consists of a photocathode DC electron gun, four superconducting cavities at 1.3 GHz (one 1-cell and three 2-cell cavities), and five solenoid magnets. These components are illustrated in Fig. 3 together with their positions and optimized parameters [8]. In this simulation, we optimized the following parameters: the initial beam profile distribution, the RF field amplitude and phase of the 1-cell and 2-cell cavities, the solenoid magnetic field, the distances between the gun and the 1-cell cavity and between the 1-cell cavity and the first 2-cell cavity. The initial macro-particle distribution is assumed to be parabolic in shape (P-1 in Fig. 3). After the electron gun, the bunch length increases due to space charge effects and consequently, the correlation coefficient increases. At the 1-cell cavity, the bunch tail has greater acceleration, which results in a decreased bunch length. The head of the bunch is merged in the middle part, while the tail particles do not merge with the middle particles. The macro-particle distribution changes in shape from a parabola to a triangle (P-2). By choosing appropriate phase and amplitude of the RF field at the 1-cell cavity, we can focus the bunch tail and defocus the bunch center . Thus, the charge density at the bunch tail can be increased to 15 times that at the bunch center. This distribution is maintained up to the entrance of the

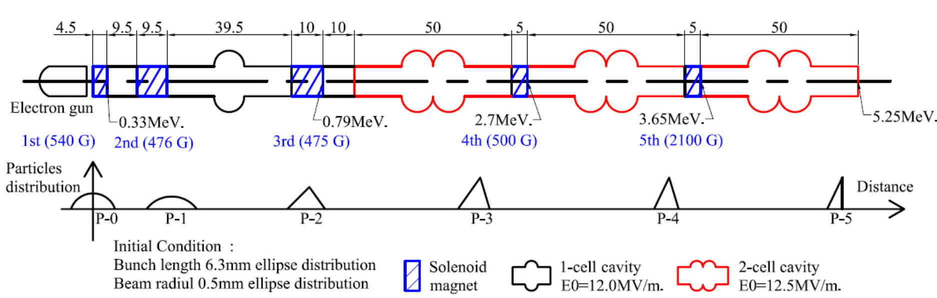

Figure 3 : Injector model parameters and element positions

first 2-cell cavity. After passing through this cavity, the shape of the charge density distribution becomes almost parabolic again while the bunch length remains nearly constant. The electron energy eventually reaches 5 MeV at the exit of the injector. The change in correlation coefficients is shown in Fig. 5, where run-away particles were not included in the caluclation. The correlation coefficient decreases from the 1-cell cavity to the first 2-cell cavity as a result of the high charge density at the tail. Thus, we can line up the slices again and obtain a small projected emittance. In order to calculate the absolute values of normalized emittance, we used PARMELA Ver 3.3 [9] and obtained a value of ~0.10 μm.

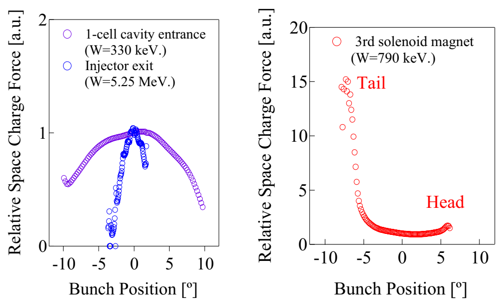

Figure 4 : Relative space charge distribution in a bunch.

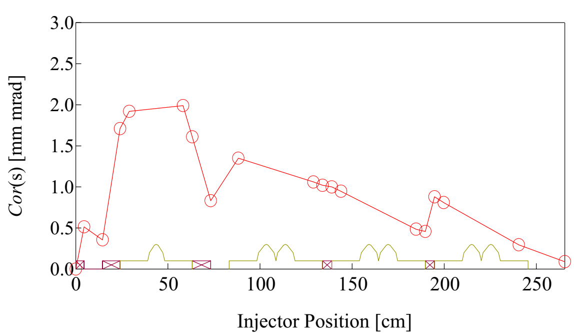

Figure 5 : "correlation coefficient" in the injector position.

DISCUSSION AND SUMMARY [8]

Changes in slice emittances are shown in the *aa'* space in Fig. 6. The initial beam is assumed to be on the horizontal axis. After emerging from the electron gun, the projected emittance becomes larger as the slice emittances have different orientations; further, due to the difference in transverse space-charge forces acting on the slices, it becomes butterfly-shaped (Fig. 6-1). Here, the space charge effects of the bunch center (denoted by a circle) are stronger than that of the bunch tail (denoted by a triangle). The second solenoid magnet focuses the bunch as shown in Fig. 6-2. The optimization of RF and magnetic field parameters of the 1-cell cavity further focuses the bunch tail while simultaneously defocusing the bunch center (Fig. 6-3). As a result, the charge densities of the bunch tail are greater than that of the bunch center. The strong space charge force that is produced causes the envelopes of the bunch tail to diverge, while the bunch center is focused by the third solenoid magnet. The projected emittance becomes much smaller, although there is still a slight variation in the slice orientations (a'/a) in the *aa'* space (Fig. 6-4). Then, after the beam waist, all the phase spaces of slices are lined up (Fig. 6-5). Hereafter, the correlation coefficient remains constant since β ($=v/c$) of the beam is approximately equal to unity, as shown in Fig. 6-6. Thus, we find that the emittance growth can be suppressed by positively using the space charge force of the bunched beam.

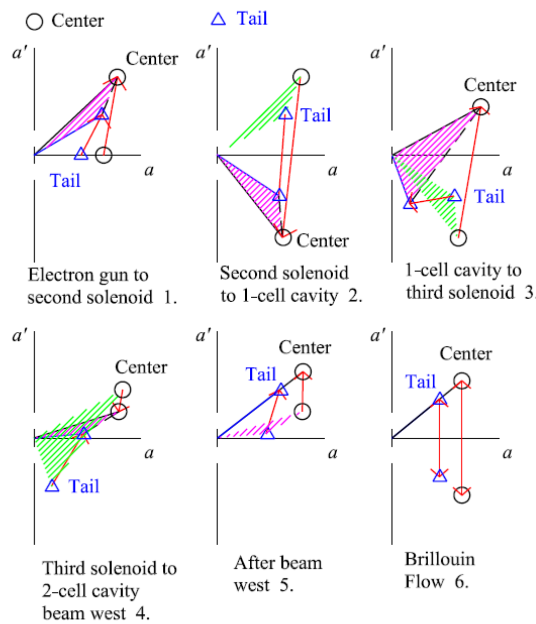

Figure 6: Compensation in *aa'* space.

ACKNOWLEDGEMENT

The authors are very grateful to Dr. R. Hajima, Dr. H. Hayano, and Dr. T Miyajima for their advice and for providing us with the injector data from PARMELA and to Dr. K Umemori and Dr. K. Saito for providing the cavity data from Superfish.

REFERENCES

[1] http://erl.chess.cornell.edu/
[2] http://pfwww.kek.jp/ERLoffice/
[3] L. Serafini and J. B.Rosenzweig, Phys. Rev. E. Vol55 (1997) 7565.
[4] T. Suwada et al., Nucl. Instr. and Meth. A557 (2006) 131-137.
[5] J.Yamazaki, et al., Proc. 6th Particle Accelerator Society Meeting, 97-99, (2009) in Japanese.
[6] H.Wiedemann,Particle Accelerators Physics I (Springer-Verlag,1999)
[7] P.Lapostolle et al., Nucl. Instr. and Meth. A275 (1996)21-40.
[8] J.Yamazaki, et al., Proc. 6th Particle Accelerator Society Meeting, 100-103, (2009) in Japanese
[9] Lloyd M. Young, LA-UR-96-1835 (1996)